

In This Issue

CHARLES STELZRIED AND MICHAEL KLEIN

In this Issue of the TMOD Technology and Science Program News, Fabrizio Pollara, suggests that using newly discovered and developed Turbo codes for Deep Space Communications is an example of a marriage made in heaven! Not only will Turbo codes improve the DSN link performance (about a dB) but at lower cost and complexity (about a factor of 10) relative to current implementations, the best of both worlds. A 'parallel' turbo code architecture has been standardized for use with the DSN and is implemented in the Spacecraft Transponder Modem (STM). Turbo codes will not only be used for communicating with spacecraft but for other important applications as well, such as cellular phones.

Jay Wyatt describes the application of the beacon monitor concept for mission operations. A proof of concept implementation was recently validated on NASA's Deep Space One (DS1) mission. With this mode of operation, a spacecraft

communicates the need for ground tracking as based on the spacecraft status using a simple tone signaling system. Future beacon monitor operation is expected to result in significant cost savings for future missions.

News from the DSN Science program is reported in two articles. The first describes how a unique combination of TMOD technology and DSN facilities is being used to study the birth of stars in our Galaxy. Steve Levin and Douglas Hofhine discuss their measurements of magnetic field strengths in cold (~10K) clouds of interstellar gas and dust using a dual-cavity Ka band maser and the beam-waveguide antenna at DSS 13. The second article features the productivity of Goldstone Solar System Radar (GSSR) observations of Near Earth Asteroids (NEAs). Lance Benner reports on the record number of NEAs successfully observed in 1999 and describes the benefits of recent GSSR hardware and software improvements at Goldstone. 

TURBO CODES AND DEEP SPACE COMMUNICATIONS: A MARRIAGE MADE IN THE HEAVENS

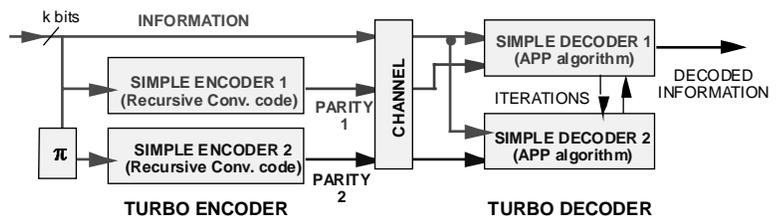
FABRIZIO POLLARA

"Turbo codes represent a quantum leap in channel coding performance for deep space applications, providing higher coding gain and much lower decoding complexity than current coding systems." (Anonymous)



WHAT IS A TURBO CODE ANYWAY?

A turbo code is a "parallel concatenation" of simple-to-decode constituent codes. Each constituent code is an encoding of a differently permuted version of a long information sequence. The archetypical turbo encoder/decoder is shown in Figure 1.



CONTINUED ON PAGE 2

Figure 1. Example of turbo encoder/decoder

For a block of k information bits, each constituent code generates a set of parity bits. The turbo code consists of the information bits and both sets of parity. The key innovation is the interleaver π preceding the second encoding. Each decoder uses the APP (a posteriori probability) algorithm to form likelihood estimates of the decoded bits, then sends these (soft) estimates to the other decoder, in the form of “extrinsic information.” The overall turbo decoder iterates between the outputs of the individual decoders until satisfactory convergence is reached.

This kind of “parallel” turbo code has been recently standardized by CCSDS under the leadership of JPL. It is also implemented in the Spacecraft Transponding Modem (STM). The Communications Systems Analysis work area has later expanded the horizon of turbo codes to “serial,” “hybrid,” and “self”-concatenations, including very low complexity “turbo-like” codes, that are only half a dB worse than the best turbo codes and are suitable for high-speed decoding.

ARE THEY ANY GOOD?

Simulations of turbo codes show that near-Shannon-limit performance is possible—better performance by 1 dB or more compared to current DSN codes (Figure 2). And, they are much simpler to decode—more than one order-of-magnitude less complex! We have also made considerable progress in developing theoretical bounds that can predict the

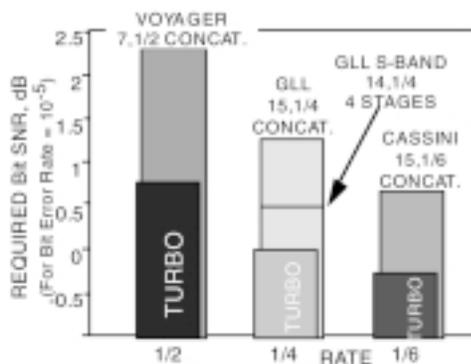


Figure 2. Old codes, new codes

performance of these (and other) codes very accurately, including the low SNR region of operation. These bounds are our mining lantern to search for new codes and to refine present ones, without lengthy and uninformative simulations. In fact, some low-rate turbo codes are so good that they put strain on the receiver, forcing it to operate at very low symbol SNR. Radio losses are no different than for conventional codes, but we plan to do better yet and essentially eliminate losses by using a coupled receiver-decoder being developed in the Network Signal Processing work area.

ONE CODE FITS ALL SIZES

Traditionally, codes have been constructed for specific block sizes or if they formed a family with block size as a parameter, they were not uniformly “good.” We have shown that turbo codes subverted even this order of things: They form a family of codes, which is near-optimal on a wide range of block sizes (Figure 3). This has

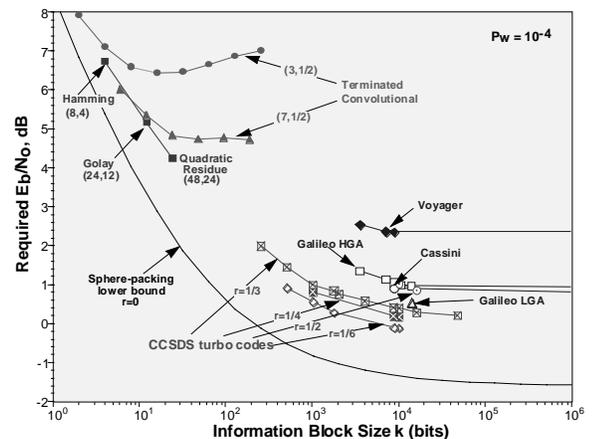


Figure 3. Performance vs. block size

important implications in applications where long latencies cannot be tolerated (engineering data, up-link, in-situ communications). The figure also shows the remarkable progress in recent coding history: Voyager to Cassini to Galileo LGA to turbo.

LOWER COMPLEXITY, HIGHER SPEED

We have developed several low-complexity “turbo-like” codes (Figure 4) that are promising for applications demanding higher decoding speeds. We have studied the complexity/performance tradeoff of these new

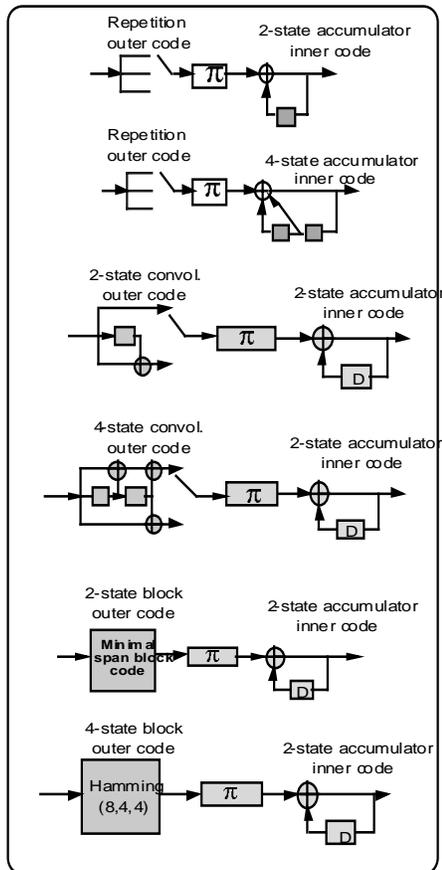


Figure 4. Turbo-like codes

codes (Figure 5), where the complexity is defined by the total number of trellis edges evaluated (forward, backward, extrinsics). This complexity measure reflects both structural complexity and iterative complexity, and is approximately technology independent. A Viterbi decoder for the (7,1/2) convolutional code has a complexity of 128 on this scale. [Reader: Can you find the complexity of the Cassini code?] The figure shows the tradeoffs possible with different classes of codes and the estimated decoding speed with current DSP or VLSI technology.

THE QUEST FOR THE DSN TURBO DECODER

We are building a turbo decoder for deep space missions to be launched in 2003 and later that will handle data rates up to 250 Kbps. The strongest code recommended by CCSDS has a block length of 8,920 information bits and code rate 1/6. This means that blocks of over 53,000 encoded symbols must be decoded every 36 milliseconds. The

CONTINUED ON PAGE 4

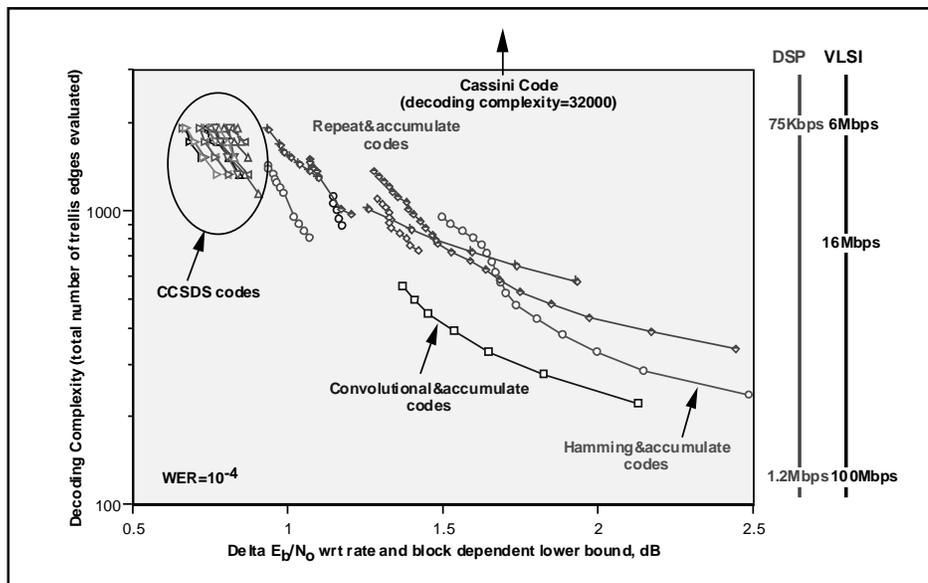


Figure 5. Complexity/Performance Tradeoffs

TURBO CONTINUED FROM PAGE 3

newest DSP chips (Figure 6) are up to the task; our decoder uses eight Texas

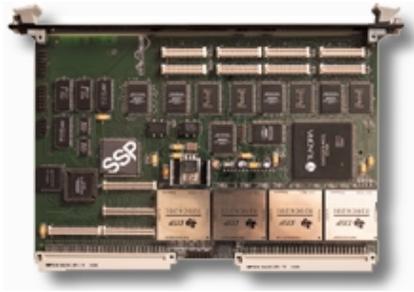


Figure 6. VME card with four DSPs

Instruments TMS320C6201 DSPs in parallel, each running at 200 MHz. Each DSP contains eight internal functional units, so it can simultaneously perform as many as six adds and two multiplies. Collectively, they deliver an impressive 12,800 MIPS.

While high-level programming languages could be used to implement the decoding algorithm, we have found that they handle the parallel architecture rather poorly. Hand-optimized assembly language, minimizing clock cycles in the inner loops, and careful memory allocation remain essential. Since the memory available within the DSP is not sufficient to hold a whole decoding block and frequent off-chip memory access is detrimental, it was necessary to design a “sliding window” algorithm that swaps the largest possible chunks of memory.

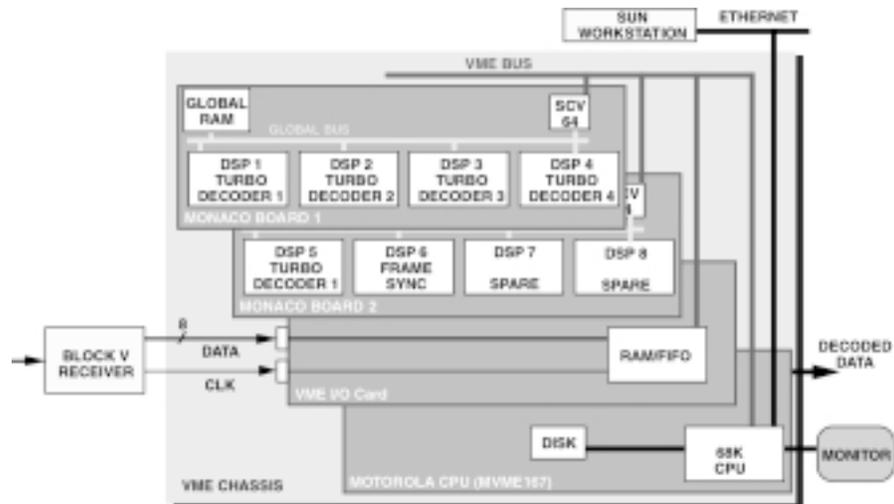
There were interesting decisions to be made in the selection of the specific decoding algorithm as well. The core step in turbo decoding computes probabilities with a multiply-and-add operation, which DSPs are particularly designed for. However, research has shown that rounding errors are less severe if logarithms of the probabilities are used instead. This maps the required multiplications to additions, while additions become a more complex operation, which can be done fastest by table lookup. With these choices, we found that a DSP can decode at about 50 Kbps and five in parallel will generously meet our data rate goal.

Because turbo codes are block codes, frame synchronization is required. This is optimally achieved by a simple correlation with a known frame synchronization marker. DSPs are excellent at this task. A single DSP can match four 192 bit sync patterns, giving optimum detection within the permitted latency. One more DSP is required to coordinate the parallel decoding and high-speed data transfers. The last DSP remains uncommitted, providing a little margin as the final algorithms are developed. (See architecture in Figure 7.)

The current decoder prototype uses a fixed number of iterations. However, we have shown that simple schemes called “stopping rules” can be used to decrease the average number of iterations while slightly improving the performance.

CONTINUED ON PAGE 15

Figure 7. Turbo decoder architecture



BEACON MONITOR OPERATIONS

E. JAY WYATT

Beacon Monitor Operations was one of twelve new technologies recently flight validated on NASA's Deep Space One (DS1) Mission. This approach to operations enables the spacecraft to inform earth when it needs assistance rather than have people on the ground continually monitor data sent from the spacecraft. More specifically, the technology enables a spacecraft to assess its own state of health and routinely indicate the *urgency* of ground intervention using a simple tone signal instead of sending data. This has a tremendous cost savings potential within NASA because sending less spacecraft health data to earth lowers the cost of conducting space missions and also decreases the burden placed on the large aperture Deep Space Network Antennas by the many missions that use them. One specific benefit of beacon monitor operations is that tone signals can use a much smaller antenna than is traditionally used for sending telemetry data.

In traditional mission operations, the spacecraft receives commands from the ground and in turn transmits telemetry in the form of science or engineering data. With beacon operations, the spacecraft sends a command to the ground (in the form of a

beacon tone) that instructs ground personnel how urgent it is to track the spacecraft for telemetry. If tracking for telemetry is required, a larger and more expensive antenna is scheduled to receive the data. This process is shown in Figure 1.

The Deep Space One mission validated the two key subsystems required to implement beacon monitor operations. One subsystem is responsible for generating the beacon tone and the other summarizes spacecraft health onboard the spacecraft. Onboard summarization is important to enable the spacecraft to gather only the most important spacecraft health data and provides capabilities for more robust anomaly detection and tone selection. Working closely with spacecraft software engineers, operations engineers, and artificial intelligence researchers, the Beacon Monitor Team designed the first comprehensive onboard data summarization system for NASA missions. Together, these two subsystems form the basis of a beacon monitor system. These subsystems are synergistic because the summarization algorithms can help determine how urgent it is to respond, which is reflected



CONTINUED ON PAGE 6

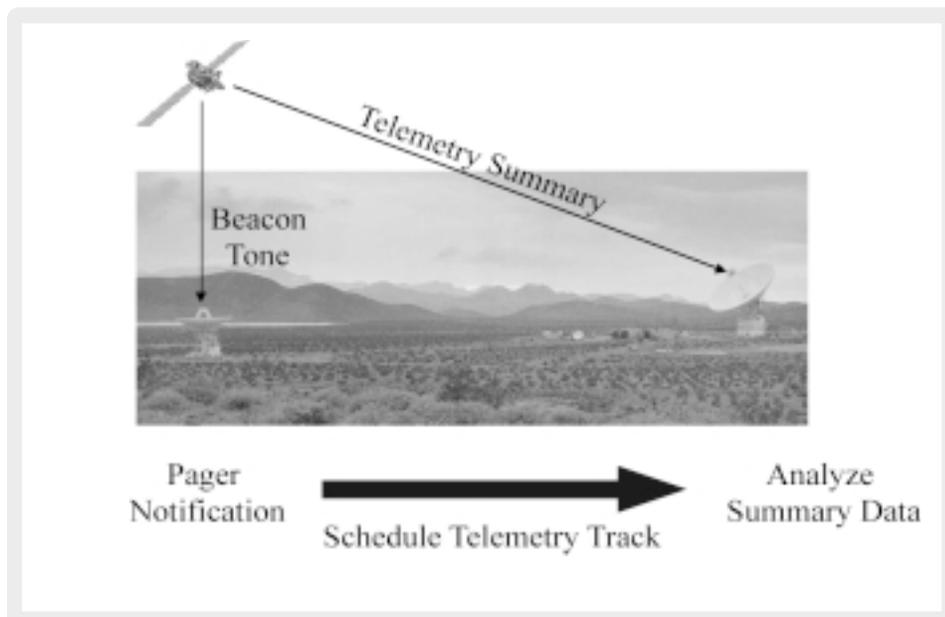


Figure 1. Operational Concept

BEACON CONTINUED FROM PAGE 5

in the beacon tone state. The summarization system also produces telemetry for downlink, but it is only sent after the tone requesting ground support is received and processed by ground personnel.

BEACON TONE MONITORING SYSTEM

Beacon tones are generated as the spacecraft reacts to onboard events. There are four tone signals and each uniquely represents one of the four urgency-based beacon messages. Tone definitions are summarized in Table 1.

Tone	Definition
Nominal	Spacecraft is nominal, all functions are performing as expected. No need to downlink engineering telemetry.
Interesting	An interesting and non-urgent event has occurred on the spacecraft. Establish communication with the ground when convenient. Examples: device reset or other transient events.
Important	Communication with the ground needs to be achieved within a certain time or the spacecraft state could deteriorate and/or critical data could be lost. Examples: memory near full or non-critical hardware failure.
Urgent	Spacecraft emergency. A critical component of the spacecraft has failed. The spacecraft cannot autonomously recover and ground intervention is required immediately. Examples: power failure or gimbal stuck.
No Tone	Beacon mode is not operating, spacecraft telecom is not Earth-pointed or spacecraft anomaly prohibited tone from being sent.

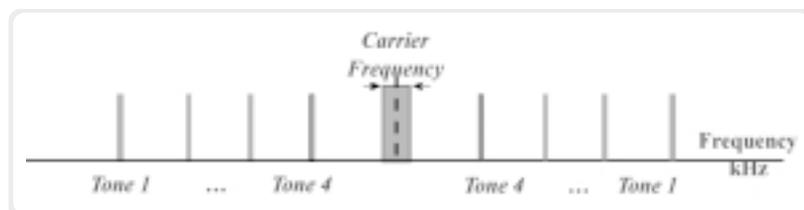
Table 1. Tone Definitions

It is important to transmit tones using a telecommunications method that has a low-detection threshold and short detection times. Ease of detection translates to lower cost operations. The tone design also allows the omni-directional antenna to be used, reducing pointing requirements and decreasing operations complexity. For ion propulsion

missions, there is also the added advantage of not having to interrupt thrusting to verify that the spacecraft is functioning correctly. The signal structure is shown in Figure 2.

CONTINUED ON PAGE 7

Figure 2. Tone Signal Structure



BEACON CONTINUED FROM PAGE 6

Each message is represented by a pair of tones centered about the carrier frequency. Tones are generated by phase-modulating the RF carrier by a squarewave subcarrier using a 90 degrees modulation angle. The carrier is completely suppressed. The resulting downlink spectrum consists of tones at odd multiples of the subcarrier frequency above and below the carrier. Four pairs of tones are needed to represent the four possible messages.

For deep space missions, tones can typically be received using smaller aperture antennas than would be required for telemetry and detection can be accomplished by providing additional functionality to existing antennas. The Beacon Monitor Team developed a detection algorithm and integrated it into the DSS13 34 meter antenna located at NASA's Goldstone Deep Space Communications Complex. Once the tone state is detected, the tone message is automatically sent to the operations team via email. The tone detection and message handling process is intended to be highly automated, robust, and inexpensive to operate. In addition to the detection software, another ground software package called BeaVis was developed by the team to track tone state and other experiment data throughout the mission. There are workstation and web-based versions of BeaVis.

ONBOARD SUMMARIZATION SYSTEM

When onboard analysis indicates that tracking is required, the corresponding beacon tone is transmitted and a summary of what has transpired since the last contact is sent when a larger aperture antenna begins tracking the spacecraft. This summary contains high-level spacecraft information, such as the number of sensors that exceed alarm thresholds, spacecraft mode and state histories, and other pertinent statistics. It also contains episode data for the culprit and causally related sensor channels around the time of anomalies or significant events. Episode data is captured at a high sample-rate since this data is likely to be very important to mission operations personnel. The summary also provides snapshot telemetry at a much lower sample

rate for all sensor and transform channels. Snapshot data is used only for rough correlation and to fill in the gaps between episodes. The last component of the downlinked summary, performance data, is similar to episode data but provides data known in advance to be of interest to people on the ground. Data around the time of a planned maneuver is an example of performance data. All of the summary algorithms are implemented in C for the VxWorks operating system.

The summary algorithms incorporate AI-based methods to enhance anomaly-detection and episode-identification capabilities. The ELMER (Envelope Learning and Monitoring using Error Relaxation) technology replaces traditional redlines with time-varying alarm thresholds to provide faster detection with fewer false alarms. The system uses a neural network to learn these functions; training can be performed onboard or on the ground. ELMER is particularly powerful because it requires very little knowledge engineering and trains the neural net with nominal sensor data. Another AI-based method produces virtual sensors by computing transforms on the existing sensor data. The transforms for DS1 can track high, low, and average values of sensors, as well as first and second derivatives. Alarm limits can be placed on these transforms and ELMER can be trained using transform data as an input. Additional transforms, if desired, can easily be defined and uplinked to the spacecraft as the mission progresses. This part of the summarization software provides a more thorough way to monitor the spacecraft for anomaly conditions and can reduce the amount of time required to diagnose problems.

EXPERIMENT RESULTS

The technology was tested during the DS1 prime mission between January 6, 1999 and September 15, 1999. Beacon tone system validation activities came first and three types of tests were conducted. There were X-band tone tests, Ka-band tone tests, and tests to verify that spacecraft software could select the

CONTINUED ON PAGE 8

BEACON CONTINUED FROM PAGE 7

correct tone based on onboard conditions. Since the current design of the Europa and Pluto missions involves using X-band beacon tones, emphasis was placed on testing at this frequency. Seven X-band tone tests were conducted to check out the functionality of tone generation (onboard the spacecraft), detection at the DSN site, and message delivery systems. These tests also characterized operational performance and obtained limits on key parameters of the system. The second type of tone test involved demonstration of the tone system operating in Ka-band. This was done to show viability of performing tone monitoring on missions only having hardware to do Ka-band signaling. The third type of tone test demonstrated end-to-end operations by showing tone selection by onboard software, tone detection, and message delivery. With the successful completion these tests, the tone portion of the technology became 100% validated.

Onboard data summarization became active on February 19, 1999 and was operated periodically until the end of the experiment. Stretching out validation over a longer time period resulted in a richer set of anomaly conditions on which to test the performance of the flight software and also afforded opportunities to fine-tune the summarization system to improve performance. Validation

criteria was met upon demonstrating that the summarization software was functionally correct and operating as expected. All of the summarization system data output products were successfully generated and downlinked periodically during the mission. Data quality was verified largely through discussions with spacecraft engineers who understand what information needs to be summarized and what data values to expect.

Detailed performance assessments began by conducting several off-line tests using ground data before the experiment was turned-on and throughout the DS1 prime mission whenever new experiment data was received. Many examples were generated to show how adaptive alarm limits can be more useful than the current state-of-the-art. One significant result was that adaptive alarm thresholds tend to track gradual trending of sensor data much tighter than static alarm limits.

Another example, shown in Figure 3, confirms that summarization can capture subtle, yet important spacecraft episodes. In ground tests, ELMER detected an unexpected heater turn-on that occurred when the

CONTINUED ON PAGE 16

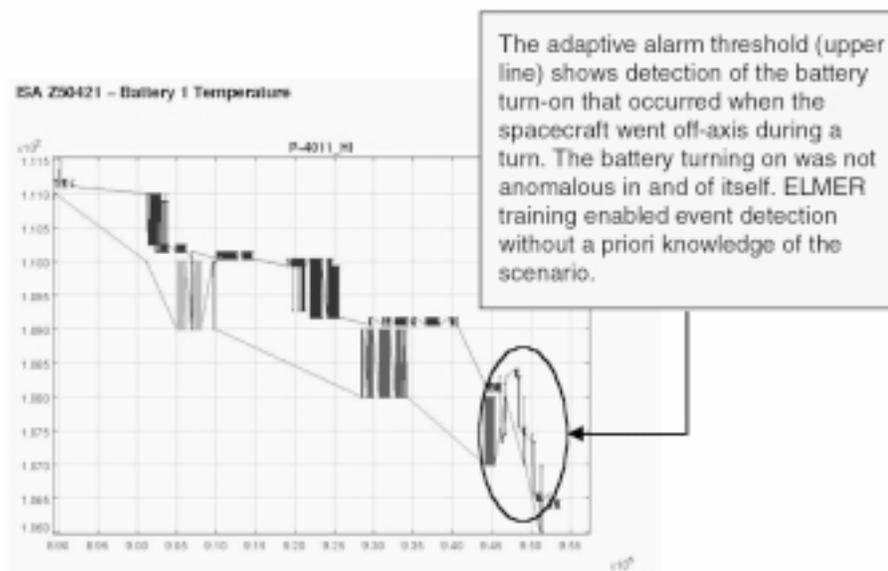


Figure 3. Adaptive Alarm Limit Anomaly Detection

MEASURING MAGNETIC FIELDS IN STELLAR NURSERIES

STEVE LEVIN AND DOUGLAS HOFHINE

With the aid of TMOD technology, DSN facilities are being used to measure magnetic fields in cold (~10 K) molecular clouds — the places where stars are born. Understanding star formation is a fundamental part of NASA's Origins theme, and magnetic fields have long been considered a critical piece of the puzzle of star formation. Measuring a 50 microGauss magnetic field from a distance of hundreds of light years is not an easy task, but a unique combination of TMOD technology and DSN resources make it possible.

BACKGROUND

Stars form from the gravitational contraction of relatively dense clumps of material (called "cores") in cold molecular clouds. The details of the process are not yet well understood, but one key piece of the puzzle is the role of magnetic fields. A significant fraction of the material is ionized, so the magnetic field can greatly affect particle motions, slowing or even preventing the gravitational contraction.

Current theories suggest that the nature, or even the existence, of star formation depends critically on the strength and geometry of the magnetic field in the cloud cores. A strong magnetic field would inhibit the gravitational contraction, while a weak magnetic field would present much less of a barrier to star formation. By measuring the magnetic field in cloud cores just before they form stars, we can gain a better understanding of the role of magnetic fields in the star formation process. To do so, we make use of the "Zeeman effect" in the CCS molecule.

In 1896, Pieter Zeeman discovered that certain spectral lines (resonant emission frequencies characteristic of specific chemical compounds) are "split" into multiple frequencies in the presence of a magnetic

field. Furthermore, the magnitude of the frequency shifts is proportional to the strength of the magnetic field. To measure magnetism at a distance, then, we need only find an emission line with a significant "Zeeman splitting", and measure the size of its frequency split.

Zeeman splitting measurements have been done many times before under a variety of circumstances, but in cold molecular cloud cores a number of complications make the measurement quite challenging. We need to use a molecule with significant Zeeman splitting and it also has to be a molecule found in the cloud cores in detectable quantities. Of the available candidates, OH, CN, and CCS are the most promising. OH has the largest Zeeman splitting, and OH measurements have been done in the past, but because OH is found nearly everywhere, with no particular concentration in the cloud cores, it is extremely difficult to separate the cloud core from its surroundings. Recent CN measurements have succeeded in hotter, denser, clouds, but CN is not found at the low temperatures and densities of interest to us, and the mm-wave frequencies of its spectral lines make the measurement difficult. CCS has been shown (largely through the use of DSN antennas) to be present at temperatures and densities ideal for isolating the pre-protostellar cores. Its Zeeman splitting is smaller than for OH or CN (about 50 Hz for the field strength expected in a typical core), but large enough to be detected with the proper equipment.

EXPERIMENTAL CONCEPT

The concept of our measurement is simple:



CONTINUED ON PAGE 10

MEASURING CONTINUED FROM PAGE 9

- Pick a pre-protostellar molecular cloud core.
- Observe the spectrum to determine the Zeeman splitting in the CCS line at 33.751 GHz.
- From the frequency splitting, calculate the magnetic field along the line of sight.
- Repeat to build up signal to noise and statistics.

In practice, the measurement is not so simple. There are a number of problems which had to be addressed, some of which are discussed below.

PROBLEMS (AND SOLUTIONS)

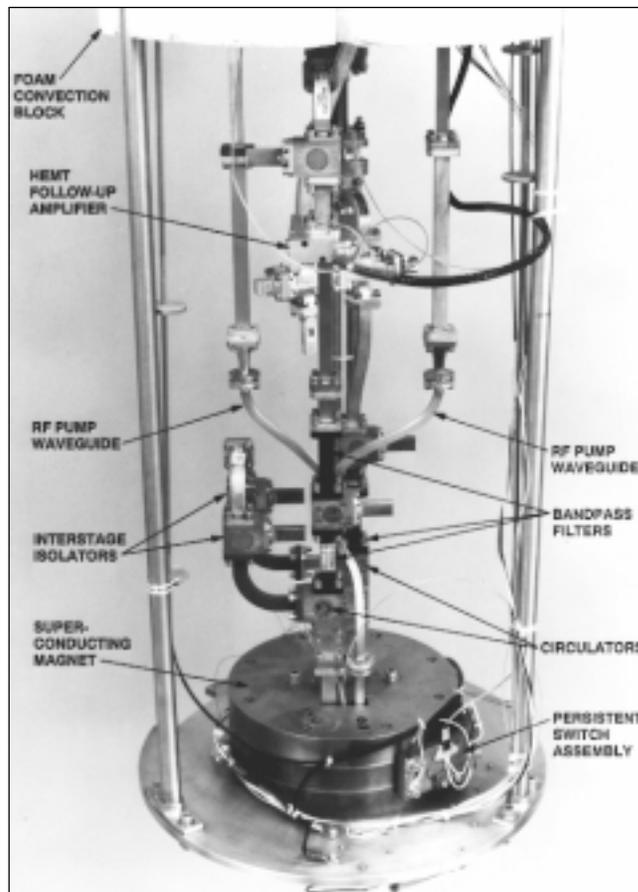
While the expected frequency shift is only about 50 Hz, the typical line width (due to the combined Doppler effects from turbulent motion of the gas and thermal motion of the molecules) is about 15 to 20 kHz. Fortunately, the Zeeman effect is polarization dependent.

When the spectral line splits, the two new lines have opposite circular polarization. For a magnetic field direction pointing away from us, the higher frequency line will have right circular polarization (RCP) and the lower frequency line will have left circular polarization (LCP). For an oppositely aligned field, the polarizations will be reversed. Thus we need only measure the RCP and LCP spectra separately, and calculate the Zeeman splitting from the difference in frequency of the RCP and LCP lines.

To measure such a small frequency shift, we need a high signal-to-noise ratio (approximately 500), requiring sensitivity at the mK level. Fortunately, we have a dual-cavity maser (See pages 806-8 in *Ruby Masers for Maximum G/Top*, by James S. Shell, et al, May 1994 Proc. of the IEEE, Vol.82, No. 5) which provides the lowest receiver temperature of any amplifier available at 33.75 GHz, shown in Figure 1.

CONTINUED ON PAGE 11

Figure 1. Dual-cavity maser and HEMT post amplifier as originally configured for the Ka-band link experiment.



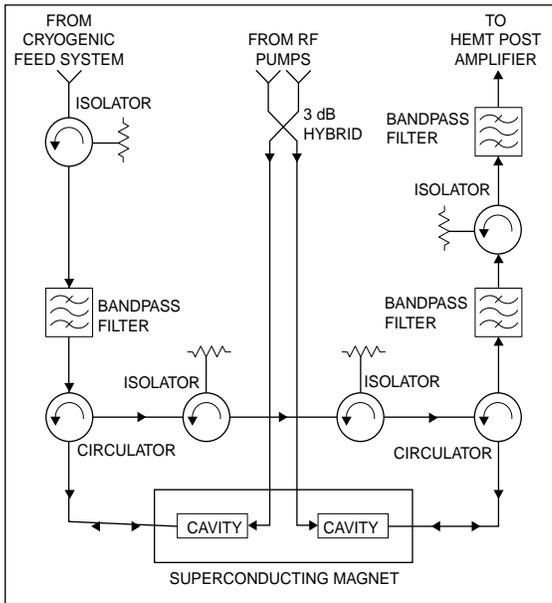


Figure 2. Schematic diagram for the dual-cavity maser as originally configured for the Ka-band link experiment.

Originally developed for the Mars Observer Ka-band Experiment (KaBLE I) at 33.67 GHz (Figure 2), the maser used the two cavities in series, providing 25 dB net gain, 85 MHz bandwidth, with an effective input noise temperature of 5 K measured at the ambient feed-horn aperture. Calibrations of the DSS-13 system prior to Mars Observer KaBLE-I telemetry experiment demonstrated system operating noise temperatures as low as 28 K at 33.67 GHz and 24.5 K at 33.06 GHz. The maser was tunable from about 33 GHz to 34 GHz. An open-cycle liquid helium dewar was used to provide temperatures as low as 1.5 K for cooling the maser.

The maser, dewar, and feed system were modified (Figure 3) to enable simultaneous reception of RCP and LCP signals at frequencies near 33.75 GHz. The extensive modification and repairs were done at the DSN's Barstow Complex Maintenance Facility (CMF) by the specialists who service operational cryo-cooled low-noise systems for the DSN. Installation, calibration and operation at DSS-13 were accomplished by the DSS-13 team, with some assistance from CMF and JPL personnel.

Each cavity maser is a single wavelength, 1.27 mm x 2.54 mm x 3.38 mm ruby dielectric resonator, mounted into a pump waveguide, and extending a small distance into a signal

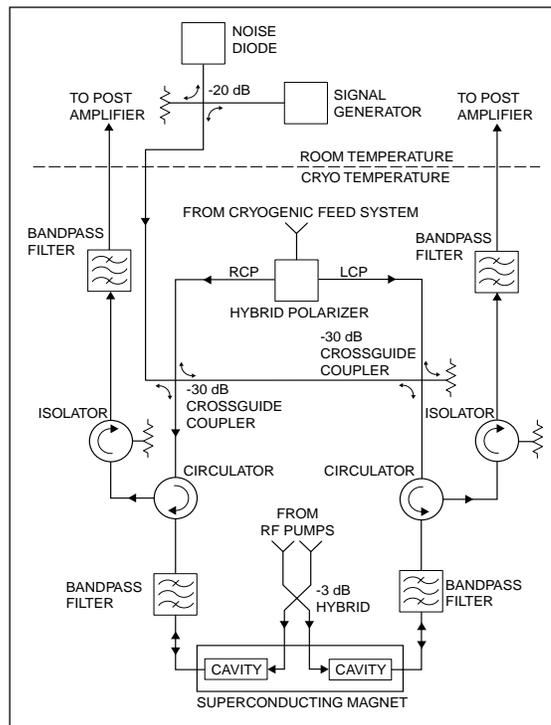


Figure 3. Schematic diagram for the dual-cavity maser as reconfigured for the Ka-band link experiment.

waveguide. A 1.25 T (12,500 gauss) superconducting magnet is used to produce Zeeman splitting in the ruby, enabling a 33.75 GHz maser, when cooled below 2 kelvin and excited with a 69.5 GHz pump energy. Tuning controls are used to adjust the gain of each cavity maser to a value near 17 dB. One cavity is used to amplify RCP signals and the other to amplify LCP signals. A cooled polarizer provides both polarizations to the two masers from a single feed horn that extends from within the dewar (near 2 kelvin) to the ambient interface at the top of the dewar. A second stage of RF amplification (a HEMT at room temperature) follows each cavity maser, adding about 8K to the system temperature but providing additional gain to allow heterodyne amplification and mixing to lower frequencies. Depending on weather, the atmosphere and antenna add another 20 to 50 K, resulting in a system operating noise temperature near 35 K with the antenna pointed at the zenith, in clear dry weather. Using this system, we can achieve the required sensitivity in 10 to 100 hours of

CONTINUED ON PAGE 12

MEASURING CONTINUED FROM PAGE 11

observation. The level of automation available at DSS13 allows a program of observation which makes extensive use of the antenna without a large drain on the station resources.

In any real system, various parameters (gain, offset, pointing, atmospheric emission, Doppler corrections, etc.) will change with time, potentially affecting the measurement. We can avoid most of these problems by measuring RCP and LCP strictly simultaneously. With a dual-polarization feed and the dual-channel maser, we combine both polarizations into the Wide Band Spectrum Analyzer (WBSA), which has 19 Hz resolution and 20 MHz bandwidth, measuring RCP and LCP spectra exactly simultaneously.

Molecular clouds have velocity structure, which translates to frequency structure (because of the Doppler effect), so any difference in pointing between RCP and LCP could result in a measurement error. To handle this difficulty, we map the molecular cloud, and measure the antenna pointing extremely accurately. At 33.75 GHz, the DSS13 34m beam waveguide has about a 0.001 degree pointing difference between RCP and LCP, which is azimuthally dependent. This difference is large enough to require calibration and correction, but not large enough to prevent the observation.

No two instrumental components (e.g., amplifiers, mixers, cables, etc.) are alike. Thus each presents a potential spurious difference between LCP and RCP spectral lines. To handle this problem, we combine the signal paths as early as possible, so that RCP and LCP share identical components for much of the system. This is accomplished by mixing the two polarizations with slightly different LO's, and then combining them at the antenna, before the fiber-optic link to the control room and WBSA. In addition, we subtract spectra with the antenna pointed off source, so that any effects which do not change between the two pointings will cancel out. Further, we note that only frequency differences are relevant to the measurement, and in the data analysis we treat all variables except the RCP - LCP frequency difference as free parameters, so that only the relevant

frequency difference is allowed to affect the measurement. Since much of the variation in components is independent of frequency, this greatly reduces the possible errors.

Finally, one problem we cannot avoid is the fact that a Zeeman splitting measurement is only sensitive to the line-of-sight component of the magnetic field. Our solution to this problem is to make Zeeman splitting maps of as many cold molecular clouds as we can, so that we can build up a statistical picture based on the random orientation of the magnetic field.

PRELIMINARY RESULTS

As of December 1999, we have taken sufficient data on our first target (a molecular cloud designated L1498) to determine the line-of-sight magnetic field. We are still analyzing the data to reduce systematic errors, but expect to publish results in early 2000. Our current sensitivity is approximately 30 microGauss, and it continues to improve as we collect more data. The magnetic fields of interest are expected to range from 10 to 100 microGauss.

ACKNOWLEDGEMENTS

This project would not be possible without the invaluable assistance of Larry Schrader and Joel R. Smith at the CMF, Jim Shell and Bob Clauss at JPL, and George Farner at DSS-13. 

GOLDSTONE RADAR OBSERVATIONS OF NEAR- EARTH ASTEROIDS IN 1999



LANCE A. M. BENNER

INTRODUCTION

1999 has been an excellent year for Goldstone Solar System Radar observations of near-Earth asteroids. As of early-November we have detected echoes from seven asteroids, none of which had ever been detected before, and six of these campaigns were short-notice “target-of-opportunity” observations of asteroids that had just been discovered. The total of seven this year exceeds the previous record of six newly-detected asteroids per year, which was set in 1996, and the number of target-of-opportunity detections doubles the previous record of three that was set in 1991 and matched in 1998. The all-time record for total Goldstone asteroid radar detections (new asteroids plus previously known objects) in a single calendar year is nine (also set in 1996), a record that we may exceed by the end of December. Radar detections of near-Earth asteroids at Goldstone since the spring of 1999 have occurred at the rate of about one per month.

The Principal Investigator in this research is Dr. Steven J. Ostro (JPL). Other JPL scientists who play key roles are the author,

Dr. Raymond F. Jurgens, Dr. Jon D. Giorgini, Dr. Donald K. Yeomans, and Dr. Martin A. Slade.

Table 1 below lists the asteroids detected at Goldstone in 1999 and their close approach distances. Delay-Doppler radar images of these objects will be used to reconstruct their three-dimensional shapes, which will significantly improve our understanding of their surface morphologies and geology, rotation states, surface roughnesses, surface reflectivities, surface bulk densities, compositions, and orbits.

The most extensive asteroid observing campaign conducted at Goldstone thus far in 1999 was for 1999 JM8, which we observed over a three-week span in late July and early August. Below I discuss preliminary results for 1999 JM8 and then I conclude with a brief outline of future prospects.

1999 JM8

The Goldstone observations of 1999 JM8 are among the best asteroid radar observations ever conducted. The delay-Doppler images

CONTINUED ON PAGE 14

Asteroid	1999 Month of Detection	Distance (AU)	Distance (km)	Lunar Distances
1992 SK	Mar	0.056	8.4E6	21.5
1999 FN19	Apr	0.021	3.1E6	8.0
1999 GU3	Apr	0.029	4.4E6	11.3
1999 FN53	May	0.059	8.9E6	22.8
1999 JM8	Jul-Aug	0.057	8.5E6	21.8
1999 NW2	Jul	0.016	2.4E6	6.3
1999 RQ36	Sep-Oct	0.015	2.2E6	5.6

Table 1: Detected asteroids in 1999

ASTEROIDS CONTINUED FROM PAGE 13

place about 10,000 pixels on the asteroid with spatial resolution as fine as 19 meters/pixel. These are among the highest resolution images ever obtained for any asteroid.

The images reveal that 1999 JM8 is an irregularly-shaped object that has an average diameter of about 3.5 km. Many impact craters between 100 meters up to about 1 km in diameter are evident, and there is another large concavity that does not appear to be a crater that is not yet understood. Portions of the surface are quite angular but other regions are, to first order, rounded.

The radar images indicate that 1999 JM8 has an unusual and very slow rotation state that resembles that of a football after a botched pass. The images suggest that the asteroid rotates about once per week, although much more data analysis will be necessary to thoroughly understand the rotation. The rotation of 1999 JM8 is strikingly similar to that of asteroid 4179 Toutatis, which was imaged by Goldstone in 1992 and 1996. This irregular rotation has been seen in only a few asteroids and it is thought to originate from collisions with other objects.

The radar detection of 1999 JM8 substantially improved our knowledge of its orbit, which has been classified as potentially hazardous by the International Astronomical Union, due to the proximity of the orbit to that of Earth and due to the asteroid's size, which is among the largest known objects presently classified as "potentially hazardous." Based on radar and optical astrometry, it is now clear

that 1999 JM8 will not approach Earth again as close as it did in 1999 for at least 1000 years.

The first Goldstone detection of 1999 JM8 occurred on July 18, the same day that newly discovered asteroid 1999 NW2 was also detected for the first time (about 6 hours after 1999 JM8). Those two detections set a record for the shortest time interval between the first radar detections of two newly discovered asteroids. The previous such record was about two days, which was set in April with the Goldstone detections of echoes from 1999 FN19 and 1999 GU3. The radar detection of 1999 NW2 came only three days after the discovery of that object was announced, an interval that also established a new record.

THE FUTURE

The Goldstone Solar System Radar has been optimized in recent years for observing near-Earth asteroids. A quasi-optical rf switch was installed on the feedcone to enable rapid transfer between transmit and receive modes, which reduced the switching time from about 20 seconds to about 1 second, an improvement that significantly increased the time available for acquiring data. The new switch has permitted monostatic observations of asteroids and other targets (such the SOHO spacecraft in 1998) that are closer to Earth than were previously observable and it has effectively eliminated lost observing time due to equipment problems associated with transmit/receive switching equipment. Concurrently, new software has been

CONTINUED ON PAGE 15

Goldstone radar images of recently discovered asteroid 1999 JM8 during its close approach to early in late July and early August. The Goldstone images were obtained on July 28 (Figure 2) and on August 1 (Figure 3). The radar illumination is from the top and the asteroid is rotating clockwise. These images have vertical resolution of 38 meters and 19 meters per pixel, respectively. The circular feature near the top center of the August 1 image is thought to be an impact crater about 1 km in diameter

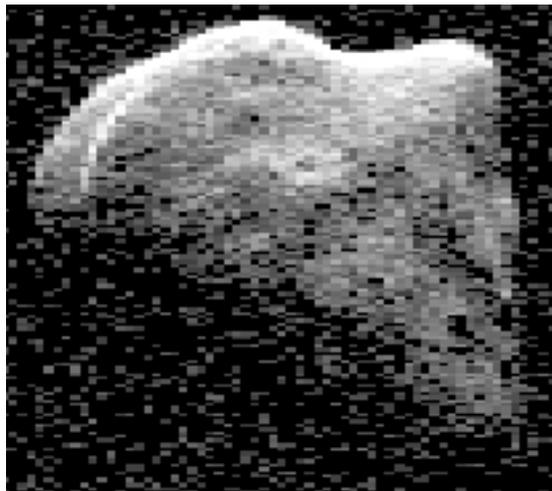


Figure 2. JM8, July 28



Figure 3. JM8, August 1

A BRIGHT FUTURE

Turbo codes are about to be deployed in applications as diverse as deep space communications and cellular phones. They brought about a revolution in coding that is forcing textbooks to be re-written. But there is more in store. In the shorter term, we envision applications where turbo codes are combined with high-level modulations to achieve high spectral efficiency. In fact, we have already demonstrated that it is possible to design codes at less than 1 dB from channel capacity even for 2, 3, and 4 bits per channel use. We will see higher speed decoders based on a universal soft-input soft-output ASIC module, which can be used in many different configurations (parallel, serial, etc.). Spaceborne decoders are in the works too. A long-term dream, where we are already making substantial progress, is the analog turbo decoder, which will be much faster and much less power hungry. Should we start thinking about molecular electronics turbo decoders?! 



developed that automatically controls the transmit/receive cycling, which was previously performed by hand by the telescope operator. Other recent improvements include a new continuous wave (CW) data acquisition and real-time display system, upgrades to the On-Site Orbit Determination (OSOD) software that are used to generate near-Earth asteroid ephemerides during the observations, and improvements to delay-Doppler data reduction and analysis software.

These investments have clearly paid off as short notice observations of new targets are likely to constitute the majority of asteroid radar research at Goldstone for the foreseeable future due to the recent acceleration in the rate of near-Earth asteroid discoveries by the optical search teams and the expected increase in that rate as new searches come online and as existing searches expand. Thus, an increasing number of excellent opportunities

to image near-Earth asteroids will occur at Goldstone in coming years in which the scientific return will be outstanding. 

BEACON CONTINUED FROM PAGE 8

spacecraft solar panels went off-axis during a spacecraft maneuver. Since ELMER trains across multiple parameters using nominal data, the summarization system detected this event without explicit a priori knowledge of the scenario.

CONCLUSION

Validation of the beacon monitor operations technology was an important milestone because it met a mission requirement that the technology be demonstrated prior to use on planned NASA missions to Europa and Pluto. In the meantime, the DS1 Extended Mission has requested the technology because of the cost savings that it can bring to the mission. The Beacon Monitor Team is supporting this request by increasing the level of automation in the tone detection process and providing the necessary updates to the flight software. In the broader view, the NASA culture is evolving to become more accepting of highly autonomous mission designs and there is also a realization that substantial levels of autonomy will be required in order to achieve some of the difficult mission challenges that lie ahead. Beacon operations is in part about leveraging these recent advances while also providing some added functionality in order to conduct these missions more cheaply and in some cases, more reliably. For more information, please consult our website: <http://eazy.jpl.nasa.gov/beacon>. 

ON THE WEB

The TMOD Technology program description, task plan and related features such as the *TMOD Technology and Science Program News*, are located at:

<http://tmot.jpl.nasa.gov/index.html>

DISTRIBUTION

To have your name added to or deleted from the *TMOD Technology and Science Program News* distribution list, call 4-9071.

The *TMOD Technology and Science Program News* is a publication of JPL's Telecommunications and Mission Operations Directorate (TMOD). The TMOD Technology Program is managed by Jim Lesh and the Science Program by Michael J. Klein.

Managing Editor Charles T. Stelzried
Associate Editor Christopher A. Weaver
Layout Presentation Media, Inc.